JOURNAL OF MATERIALS SCIENCE 8 (1973) 265–278

Deformation and fracture of synthetic α-quartz

N. E. W. HARTLEY, T. R. WILSHAW
Materials Science Laboratory, School of Applied Sciences, University of Sussex, UK

The deformation and fracture properties of synthetic α-quartz crystals were measured using hardness, pre-cracked bend and Hertzian tests over the range 20 to 545°C in air and dry nitrogen. The resistance to fracture decreases significantly with increase in temperature and is orientation-dependent (becoming very small as the inversion temperature is approached), while the microhardness remains relatively insensitive to temperature and environment. These effects are interpreted in terms of the moisture content of the environment and the intrinsic water content of the crystals.

1. Introduction

The deformation and fracture behaviour of quartz is of fundamental interest to the earth sciences and many branches of technology. Previous work has centred either on the deformation problem, using hardness tests [1–3] and compression tests [4–11], or on the fracture behaviour [12–14]. The outcome of these studies has been the identification of some of the parameters which influence the mechanical behaviour of quartz, such as impurity content [2, 3] (particularly water [4, 5]), chemical environment [6], temperature [7, 8] and loading rate [5, 9]. The role of these variables is often difficult to measure and even more difficult to explain in terms of a fundamental model. Although quartz is readily obtainable in the form of large single crystals it is nevertheless a difficult material to work with because, in addition to being subject to the variables listed above, it is anisotropic with some tendency to cleave.

This paper is an attempt to quantify the effects of many of these variables and thereby to determine their relative importance. The approach to the problem has been to separate as far as possible fracture from deformation in order that a study of each might be made. Synthetic α-quartz was chosen as the principal material. The temperature range from room temperature up to 545°C was investigated using Vickers hardness indentation (deformation) and Hertzian contact loading (fracture). The results are discussed with particular reference to the hydrolytic weakening model of quartz [5].

1.1. Structure and physical properties of quartz

The standard reference work on the structure and properties of quartz and the silicates is the book by Dana [15]. A concise account has recently been given [8] of the relationship between the high pressure/high temperature phases of silica, one or more of which may be produced during hardness indentation [3]. α-Quartz crystallizes with a hexagonal lattice which exists up to 573°C at atmospheric pressure, and has no centre of symmetry and no plane of symmetry. The primary structural unit is the SiO_4 tetrahedron in which one silicon atom sits interstitially between four oxygen atoms. The extension of these units in three dimensions produces a framework structure in which each of the oxygen atoms at the corner of a tetrahedron acts as a link between adjacent tetrahedra [15].

Of the many twinning modes that can exist in quartz [15], twinning by a 180° rotation about [0001], is the only mode which may be produced as a result of mechanical forces [1]. This is known as the Dauphiné twin and is referred to later in the discussion of Section 4.

Synthetic hydrothermally grown quartz crystals were obtained from the Sawyer Research Corporation, USA. Mass spectrometry revealed that there was a small difference between the metallic impurity content of synthetic and Brazilian quartz specimens (Table I). Generally, synthetic quartz has a higher intrinsic water content than natural quartz [8] and this was

TABLE I Mass spectrometry analysis of impurities in quartz (ppm)

	I	Br	K	Cl	Al	Mg	Na
Brasilian	50	100	40	250	60	40	120
Synthetic	1	1	15	50	50	60	120

found to be the case with the Sawyer crystals from estimates of i.r. spectra [16]. Hydrothermally grown quartz crystals have a characteristic extremely low dislocation density.

The crystals were oriented by Laue back-reflection and were then cut up on a diamond saw to within $\pm\frac{1}{2}°$ of the required crystallographic plane. They were then subjected to an abrasion treatment for Hertzian testing, or were pre-cracked for fracture toughness testing. In this series of experiments the three mutually perpendicular planes shown schematically in Fig. 1 were studied. The three cuts correspond to the conventionally denoted X, Y and Z cuts which identify with the planes $(11\bar{2}0)$, $(1\bar{1}00)$ and (0001) respectively.

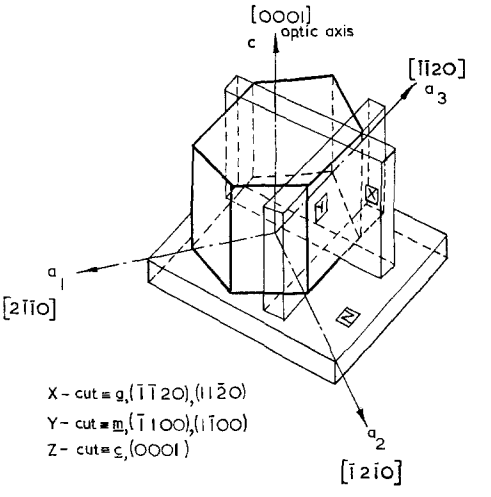

Figure 1 Schematic diagram of the orientation of the three principal cuts with reference to the quartz crystal lattice.

2. Deformation

The most convenient method of determining the deformation behaviour of strong brittle solids is the microhardness test. An indenter of known geometry, e.g. a Vickers diamond pyramid or Knoop indenter, is forced into the surface under a known load, and the depth of penetration is directly related to the resistance to flow of material around the indenter. Microhardness data have been interpreted in terms of the flow stress [17] and more recently in terms of the operative slip systems [18]. Very brittle materials such as glass [19] and quartz [1–3] will permanently deform even at room temperature under the action of an indenter. A basic question arises as to what physical mechanism or mechanisms are responsible for the permanent displacements created by a microhardness indent.

The object of the hardness tests in this work was to determine the effect of temperature, orientation and environment on the resistance to plastic deformation. Since fracture is essentially a limiting stage in the plastic deformation process it is important to determine the relationship between the two phenomena.

The tests were carried out on mechanically polished surfaces under loads ranging from 10 to 100 *g*. Visible cracks appear at the corners of indentations in quartz at loads above 30 *g*, but the presence of cracks did not affect the hardness number. The load applied during identation was maintained for 30 sec.

It was not possible to detect a difference in hardness between the planes $(11\bar{2}0)$, $(1\bar{1}00)$ and (0001) although Taylor [20] is quoted as finding $\{10\bar{1}0\}$ harder than (0001), and Westbrook's data show that the prism plane is about 15% harder than the basal plane. Since the specimens were polished before testing it is possible that residual stresses were introduced into the surface, although no evidence for this was found. The results of hot-hardness tests on a well polished *c* (0001) specimen are shown in Fig. 2. Also included are the results obtained when hot nitrogen was flushed over the surface of the specimen. (The nitrogen environment was designed to compare with the nitrogen conditions described in Section 3.3.) The results of Westbrook [1] are represented by the dashed line.

2.1. Deformation mechanisms in quartz

There are four ways by which strain may be accommodated during indentation: (i) by dislocation motion away from the indented region, (ii) by densification, (iii) by twinning, or (iv) by a microfracturing process such as that proposed by Brace [2] for quartz. Densification has been shown to occur under indentations in glass [21]. However, in quartz which is more dense than glass and whose bonds are directional and partly ionic [22] it is doubtful that densification is primarily responsible for accommodating the

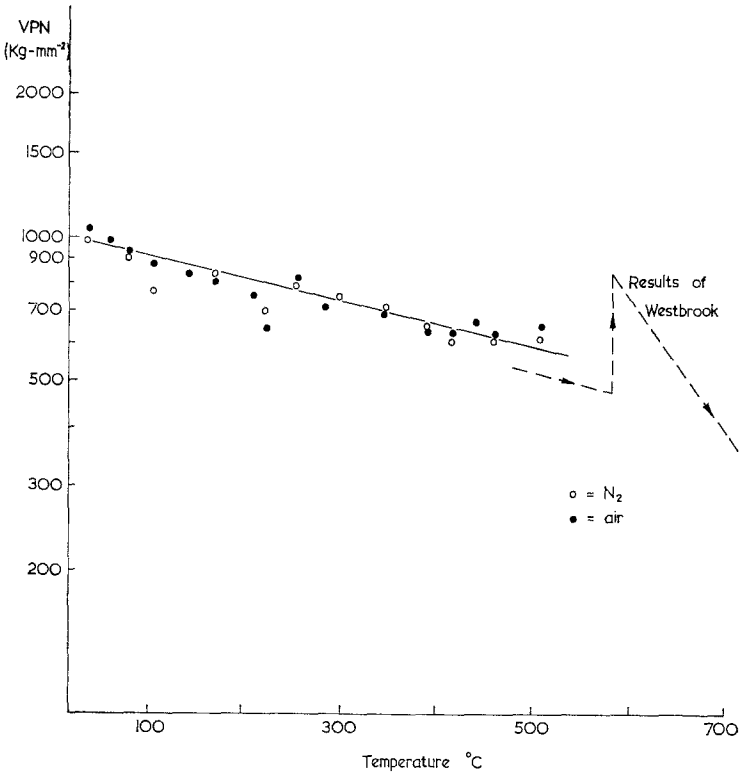

Figure 2 Vickers hardness on (0001) synthetic quartz plane for air and nitrogen environments as a function of temperature.

large strains (about 8% [23]) associated with indentation. Firstly, extremely high pressures are required to form either of the denser forms of quartz (coesite and stishovite) and secondly there is evidence that even under suitably high conditions of pressure and temperature the transformation to coesite is thermodynamically unfavourable since the time required is long at low homologous temperatures [24]. Nadeau and Brace have considered the case for the formation of coesite below an indenter [2, 3]. Although microcracking and twinning do occur under most indentation conditions these processes do not accommodate sufficient amounts of displacement to warrant serious consideration as the principal deformation modes either.

By a process of elimination, therefore, the most likely mechanism is plastic deformation by a slip process produced by dislocation motion. The recent analysis of Brookes *et al* [18] is based on the critical resolved shear stress acting below a Knoop indenter, and the observed directional anisotropy in hardness correlates well with the predicted contributions from the established slip systems of several crystals. However, it has not been demonstrated to date that dislocations on slip planes are responsible for accommodating displacements in quartz. If the ability of quartz to deform under hardness impressions is predominantly determined by dislocation motion, then it is probable that the slip which takes place is non-crystallographic. The suggestion that indentations are formed as the result of plastic flow involving dislocations has been made by Nadeau [3]. Analysis of the results of Knoop hardness tests on quartz [25, 27] shows that the small degree of directional anisotropy in hardness which exists in quartz cannot be assigned to variations in the critical resolved shear stress on crystallographic slip planes of low index.

A thermally activated softening phenomenon was observed by Griggs and Blacic [4] from uniaxial compression data obtained over a range of temperatures. The onset of weakening occurred at a specific temperature dependent on the intrinsic water content of the crystals (Fig. 3). Although the fundamental mechanism has not been clearly established, the hydrolytic weaken-

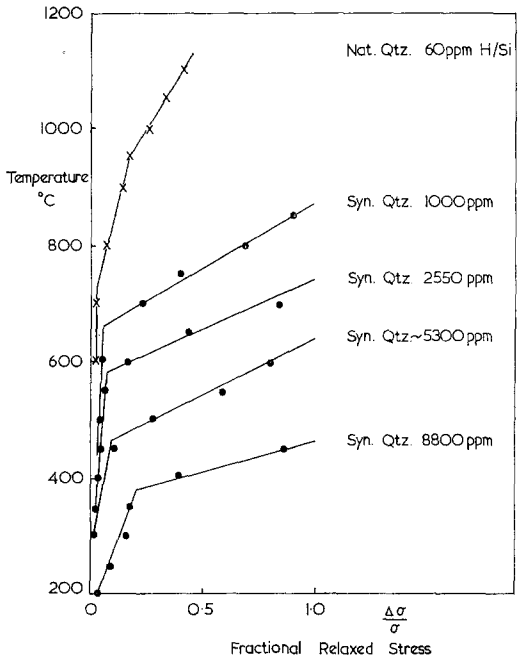

Figure 3 Fractional stress drop ($\Delta\sigma/\sigma$) as a function of temperature for synthetic and natural quartz single crystals with various intrinsic water contents. Specimens held for 20 min at successive 50°C increases in temperature (from Fig. 8, [5]).

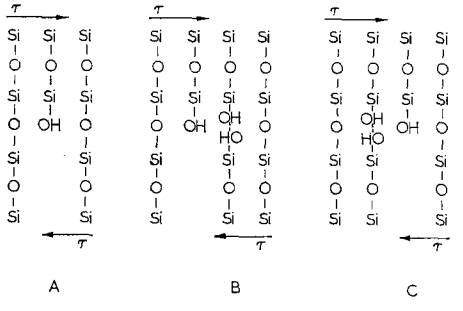

Figure 4 Schematic model of the Frank-Griggs mechanism of dislocation motion by hydrolysis and hydrogen bond exchange; A: sessile hydrolysed edge dislocation with anhydrous neighbours; B: neighbouring bridge hydrolysed by water migration; C: dislocation moves by exchange of hydrogen bond with neighbouring bridge [5].

ing model proposed by Griggs [5] is consistent with most of the major features of this phenomenon. A schematic representation of the model is presented in Fig. 4. The suggested mechanism of hydrolytic weakening is assumed to have taken place via the migration of hydrogen-bonded Si-O links of the form Si-OH . . . HO-Si through the silica lattice in such a way that dislocation kinks may move easily by hydrogen bond exchange.

It was anticipated that the hardness data would reflect any softening processes since the hardness test measures the resistance to dislocation motion. However, the temperature-dependence of the hardness (Fig. 2) shows no indication of a softening transition temperature and correlates more closely with the temperature-dependence of the elastic moduli (Fig. 5). For very hard

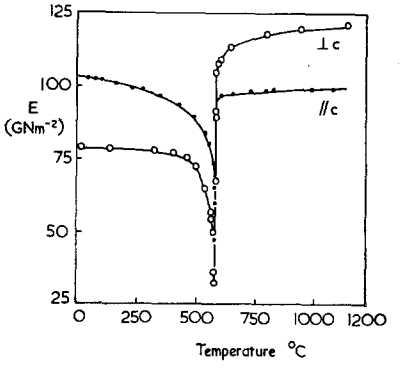

Figure 5 Temperature dependence of Young's modulus of quartz for direction perpendicular and parallel to the optic axis [0001]. (From [47]).

materials small changes in hardness are difficult to detect. In quartz it is unlikely that complete saturation by hydrogen ions will occur owing to the extremely high density of dislocations in the vicinity of an indentation. The data of Fig. 2 do not necessarily exclude the existence of hydrolytic weakening, since softening brought about by *incomplete* hydrolysis will probably not be resolved by the hardness test.

3. Fracture

The principles of basic fracture property measurement are relatively simple; a crack of known length is propagated in a specimen of known geometry under specified loading conditions. The resistance to crack propagation, usually expressed as the fracture toughness $\gamma(\mathrm{Jm}^{-2})$, or the critical strain-energy release rate $G_c(\mathrm{Jm}^{-2})$, may be calculated from the applied force which causes unstable fracture. The well-known Griffith equation is a formulation of this general statement.

There are few materials whose fracture behaviour can be exactly represented by simple theory based on the assumptions that materials

respond to stress in a linear elastic manner and that their physical properties are isotropic. Quartz has highly anisotropic elastic properties; it shows some tendency to cleave, some irreversible deformation occurs in the region of the crack tip prior to fracture [26, 27] and the fracture toughness is affected by the nature of the chemical environment, i.e. the resistance to crack propagation depends on the crack velocity [6, 27].

Some insight into the fracture behaviour of anisotropic brittle solids can be gained from the study of isolated cracks under well defined loading conditions. Two types of fracture test were used; the first utilizes large single cracks of known length fractured in three- or four-point bending [28] and is used to determine absolute values of fracture toughness. The second test – the Hertzian fracture test [29] – involves the propagation of surface microcracks and is employed here to measure *changes* in fracture toughness as affected by temperature, environment, and orientation.

3.1. Pre-cracked bend tests

The simple and effective pre-cracking technique of Brace and Walsh [14] shown in Fig. 6 was employed in this work. A rectangular slice of the Sawyer crystal of known orientation and containing a centrally drilled hole is compressed in one direction. Small cracks are made to initiate and propagate in the general direction of the compressive force. These natural cracks were not planar but followed certain cleavage planes of the $\{10\bar{1}1\}$ type. A pre-cracked prism was then prepared by sawing each side of the arrested crack (see Fig. 6a).

Pre-cracked tests of this type are now well established. The load to cause the crack to propagate, and the initial length of the crack (measured on the fracture surface), were both substituted in the appropriate equation for γ to obtain a value of 11.5 ± 1.5 Jm^{-2}, for α-quartz in air at room temperature. The only previously reported values of 0.41 to 1.03 Jm^{-2}, were obtained from Gilman tests [14] (Fig. 6b). However, if there is insufficient uncracked material ahead of the cleavage crack then the constraint afforded by the specimen is reduced. In this situation an error arises which leads to an underestimation of γ on short specimens [30]. This may account for the much greater value of γ recorded for three-point bend tests in this work and the earlier work [14] on Gilman specimens.

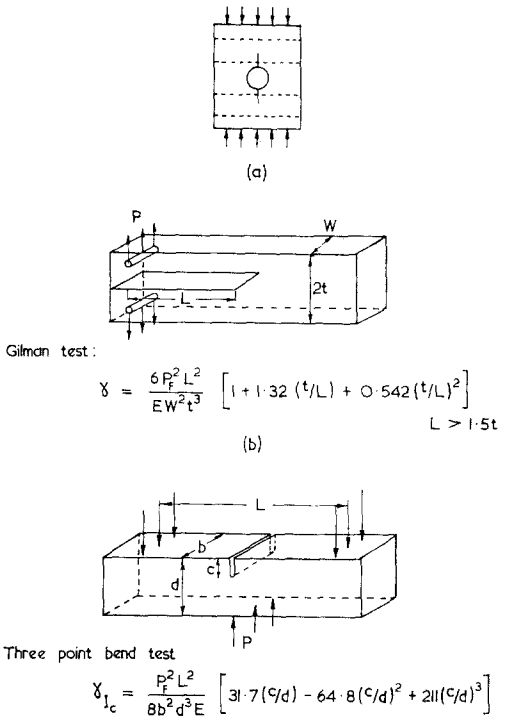

Figure 6 Schematic diagram of pre-cracking technique (a), Gilman test (b), and three-point bend test (c). In (a), the sawing directions required to produce three-point bend specimens are shown by the broken lines.

3.2. The Hertzian fracture test: theoretical background

The Hertzian fracture test is a new approach to fracture toughness testing and is convenient, simple, and entails a minimum amount of specimen preparation. The instability event is marked by the instantaneous growth of *surface microcracks* [31, 32]. The essential features involve pressing a spherical ball onto a prepared surface, until a small macroscopic cone crack suddenly appears. The critical force required to produce this crack is directly related to the fracture toughness. In several ways this test is analogous to the indentation hardness test except that it is resistance to fracture that is measured rather than resistance to deformation. That a complete theoretical treatment of Hertzian fracture in anisotropic media is not yet available is not considered to detract from the usefulness of this experimental situation.

It is instructive to examine the special case of Hertzian fracture in isotropic solids, for example glass. The development of unstable fracture is shown in Fig. 7, together with the important

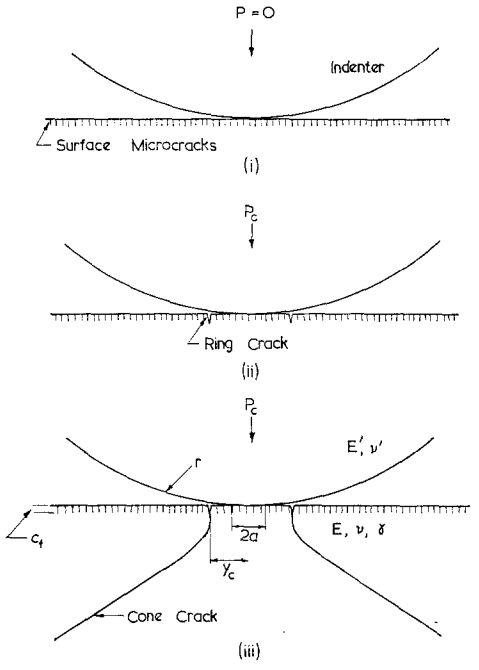

Figure 7 Schematic diagram of Hertzian instability and fracture parameters.

geometrical parameters and material properties. A spherical ball of radius r is loaded onto a surface which has been abraded in a controlled way [33] to introduce surface microcracks of effective depth c_f. The ball makes contact over a circular region radius a, related to the applied load P by

$$a^3 = \frac{4}{3}\left(\frac{kPr}{E}\right) \tag{1}$$

where

$$k = \frac{9}{16}\left\{(1 - \nu^2) + (1 - \nu'^2)\frac{E}{E'}\right\} \tag{2}$$

and E, E', ν, ν' refer to the indented medium and ball respectively, and have their usual meaning.

The near surface material outside the circle of contact experiences a tensile stress in the radial direction. On the surface itself this stress is distributed according to the relationship

$$\sigma = \frac{(1 - 2\nu)}{2}\frac{P}{\pi y^2} \tag{3}$$

This stress diminishes very rapidly with depth below the surface; however, if the microcracks c_f are sufficiently small to experience a uniform tensile stress, a simple equation for the critical fracture load P_c may be derived. Assuming that the fully developed Hertzian cone crack initiates from a crack of length c_f at y_c, and that it is equivalent to a single edge crack in tension, the fracture criterion is

$$\sigma = \frac{1}{1.12}\left\{\frac{2E\gamma}{(1 - \nu^2)\pi c}\right\}^{\frac{1}{2}} \tag{4}$$

and the critical fracture load P_c is obtained from combining Equations 3 and 4:

$$P_c = \frac{32\pi}{3(1.12)^2}\frac{kr\gamma}{(1 - \nu^2)(1 - 2\nu)^2}\left(\frac{c_f}{a}\right)^{-1}\left(\frac{y_c}{a}\right)^4 \tag{5}$$

It is then possible to calculate γ using Equation 5, by substituting all the values of P_c, c_f, y_c, and ν. However, it is not possible to measure c_f very accurately since it is only a few microns in depth within the range of applicability of Equation 5. Consequently any absolute determination of γ by this technique is subject to large errors and is very approximate [27]. Alternatively, if c_f and y_c are maintained constant, i.e. the specimen surfaces are prepared consistently, *then the fracture toughness is directly proportional to the fracture load.*

The following experiments were designed to determine the effects of temperature, environment and orientation on the fracture toughness by measuring the Hertzian fracture load.

3.3. The Hertzian fracture test: experimental

A 12.7 mm diameter tungsten carbide ball was loaded onto a carefully abraded specimen surface at a rate of approximately 10 Ns^{-1} which corresponds to a constant velocity of approach of 10^{-6} $msec^{-1}$. The instability load P_c was recorded by stopping the test as soon as the Hertzian cone crack appeared.

The surface abrasion conditions were determined from a preliminary set of tests designed to achieve maximum reproducibility in P_c within a minimum preparation time. Each specimen was lapped under a pressure of about 10^4 Nm^{-2} for 1 h using F500 (12.8 μm) SiC followed by a further hour with F1000 (4.8 μm) SiC. The abrasive grit was continuously applied as a water slurry and completely recharged every 10 min. Specimens were finally rinsed and ultrasonically cleaned in ethyl and methyl alcohol or water, and air-dried prior to testing. The majority of tests were carried out in air on a specially constructed hot-stage. Some experiments were also performed whilst enveloping the surface of the

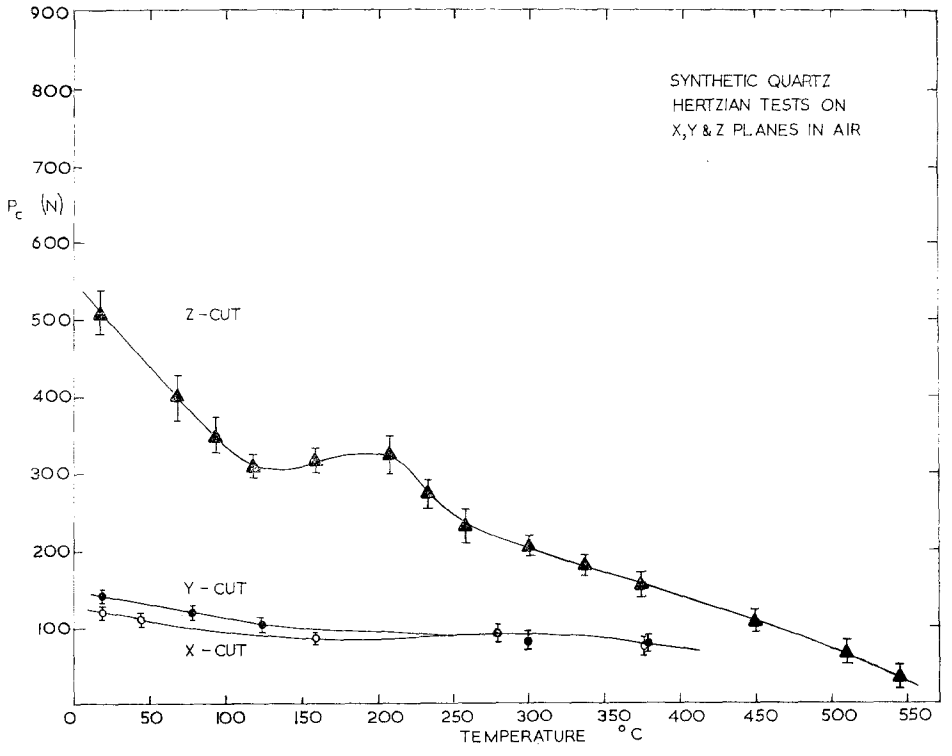

Figure 8 Results of Hertzian tests on X, Y and Z-cut synthetic quartz in air as a function of temperature.

specimen with dry nitrogen. Nitrogen was chosen because it does not react with quartz, and also because it is readily available as a nominally water-free gas. For the high temperature experiments (Fig. 9) the N_2 was heated before reaching the environmental chamber.

The spacing of the indentations was arranged so as to optimize on the amount of surface available whilst ensuring that there was no interaction from residual stress fields due to neighbouring cracks. This enabled between 12 and 36 tests to be performed on a single specimen. The Hertzian fracture load calculated from the data corresponds to a 50% probability of a cone crack occurring at that load [33]. The error bars shown in Figs. 8 and 9 represent the minimum confidence in the 50% probability value of P_c calculated from the total number of tests carried out at each specific temperature.

The room temperature results are presented in Table II along with data for soda lime glass and silica for a comparison. The results of varying temperature, orientation and environment are summarized in Figs. 8 and 9, and will be discussed in the next section.

TABLE II Hertzian fracture data (in air at room temperature).

	P_c(N)	y_c/a	ν
Soda-lime glass	450	1.37	0.23
Fused silica	250	1.40	0.184
Synthetic quartz (0001)	510	1.25	0.118
„ „ $(1\bar{1}00)$	150	1.20	0.014
„ „ $(11\bar{2}0)$	120	1.15	0.1

4. Discussion

4.1. Anisotropy

4.1.1. Crystal symmetry

For elastically isotropic materials such as glass, P_c is marked by the instantaneous formation of a complete cone crack which, on further increase in load, propagates stably down into the specimen. The extension of stable cone cracks under increasing load can be analysed to evaluate fracture surface energy [34]. With anisotropic materials the analysis is more complicated since the cone crack is often only partially complete at instability and its inclination may vary with sectioning direction. This was found to be the case even with quartz which is considered to

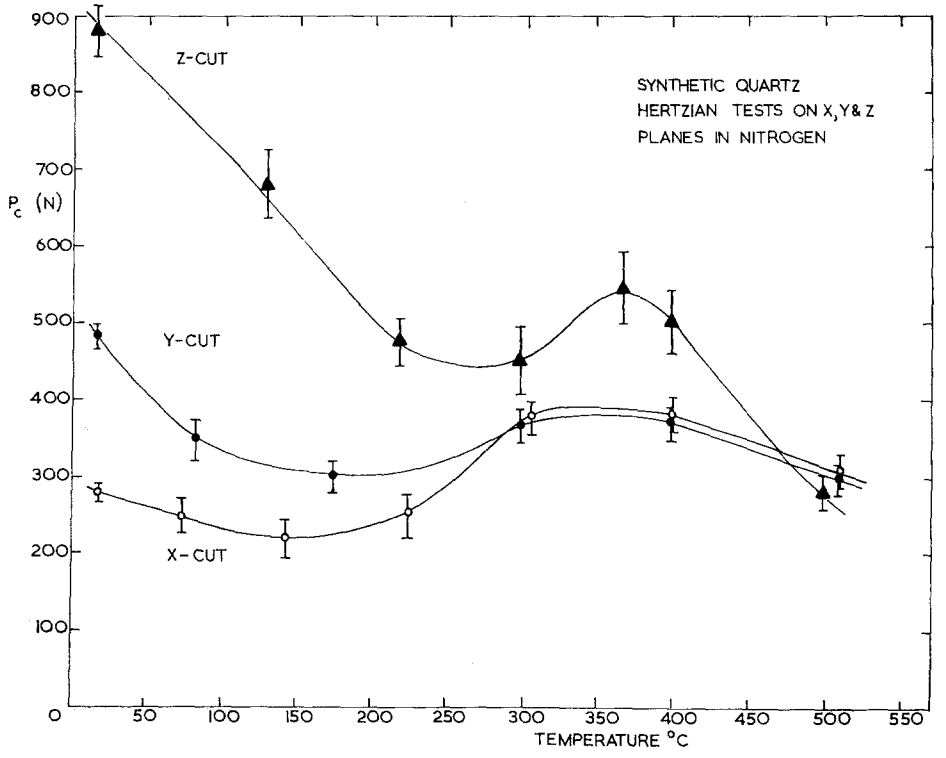

Figure 9 Results of Hertzian tests on X, Y and Z-cut synthetic quartz in nitrogen as a function of temperature.

have very low cleavage tendency. For example, on m $(1\bar{1}00)$ the indenting load had to be increased to $2P_c$ to complete a partial cone crack.

Lawn has pointed out that the indentation of crystals would result in a cone crack whose surface trace reflects the symmetry of the crystal structure [35]. Photographs of etched cone cracks on c (0001), m $(1\bar{1}00)$ and a $(\bar{1}\bar{1}20)$ are shown in Fig. 10. The "symmetry" of the crystal structure below the surface appears to be governing the shape of the indentations. This is most marked on the basal plane (Fig. 11a). Similar observations of symmetry were recorded by Schubnikov and Zinserling [12] and also, more recently, by Schlössin [36]. Schubnikov and Zinserling described the results of percussion (i.e. impact) and pressure experiments with a steel ball on sawn sections of natural quartz in some detail and claimed elsewhere (see account in [1]) to have observed a 15:1 reduction in "yield point" between room temperature and 573°C. A recent summary of their observations on cone crack morphology has been given by Brace [2]. In general our observations are in agreement with those of this early work with the exception of the ring cracks produced on $\{10\bar{1}0\}$ which failed to reveal the re-entrant characteristic depicted in their sketch (reproduced in Fig. 10d). Fig. 10a shows clearly the development of Dauphiné twins which are revealed by etching in a solution of HF. The production of twins in quartz as a result of externally applied mechanical forces* is one of the earliest observations on quartz recorded, and has been discussed in detail by Thomas and Wooster [48] and also in a recent translation of Russian work [37]. In the Hertzian fracture of quartz it is necessary to make a clear distinction between twins nucleated at the first point of contact of the indenter and the surface as a result of contact loading, and those which may occur in the bulk of the specimen from mechanical strain below the indenter. Whether or not Dauphiné twins are associated with cone crack fracture is still to be resolved. Pressure-induced Dauphiné twins extend for very large distances as revealed at the surface (Fig. 10a) and involve only small local atomic motions without macroscopic resultant. The

*Such Dauphiné twins are not normally bounded by rational twinning planes, but have irregular outlines.

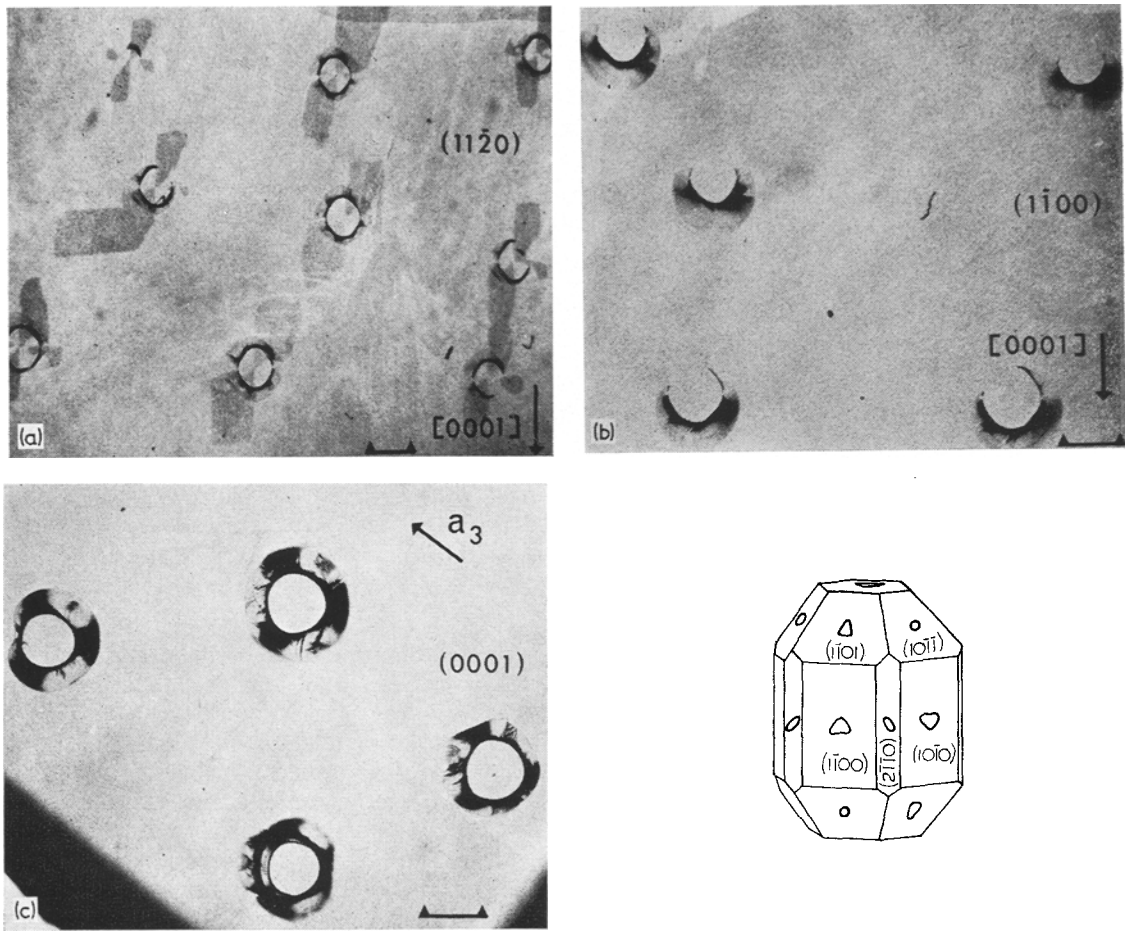

Figure 10 Photographs of cone cracks on X, Y and Z-cut planes after a 2 h etch in HF (1 + 1, 40% HF + water): (a) X-cut (11$\bar{2}$0), (b) Y-cut (1$\bar{1}$00), (c) Z-cut (0001). Marker = 1 mm. (d) Form of ring cracks produced by Schubnikov and Zinserling [12].

reason why Dauphiné twin patterns form when quartz surfaces are point-loaded is that quartz is elastically anisotropic and the formation of twins in sectors allows the imposed elastic strain to be more efficiently accommodated in the manner explained by Klassen-Neklyudova [37] and by Thomas and Wooster [48]. Schlössin, in a recent study of the static compression of α-quartz, concluded that Dauphiné twins were invariably produced "ahead of fracture" during contact loading. It is possible that the production of Dauphiné twins during point-loading contributes towards "crystallographic" indentation figures. It was not possible to establish this unambiguously from etching experiments on complete cone cracks. However, Withers has shown [38] that under laser-induced conditions of extremely high impact, local fracture in quartz shows *more* crystallographic symmetry than in the static case (Fig. 11b). This unusual observation of strain-rate sensitive symmetry appears to be the reverse of that experienced by Schubnikov and Zinserling.

For isotropic materials in which the ring crack and contact area are concentric, Equation 5 may be used to calculate γ provided y_c/a is known with sufficient accuracy. In quartz the contact area is often not centrally placed within the ring crack and therefore it is necessary to make careful observations of the point of initiation of the ring crack at instability (initiation arc). One method of establishing the position and extent of the contact area of transparent anisotropic materials is to indent through a

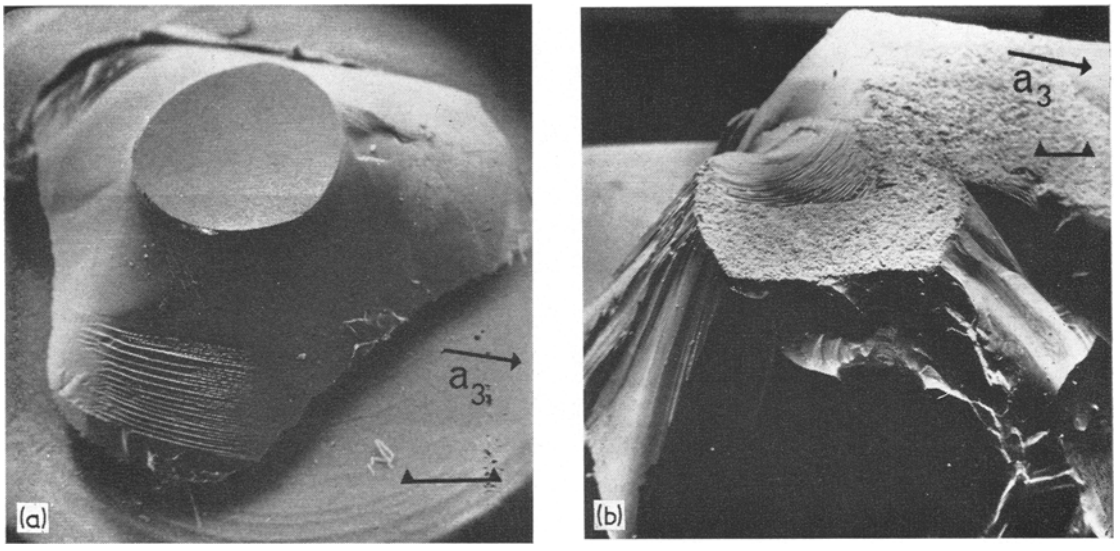

Figure 11 SEM photographs of cone cracks completely removed from (0001) specimens by milling away lower surface after fracture; (a) quasi-static loading (10 Ns^{-1}), (b) shock loading (10^7 Ns^{-1}). Marker = 0.5 mm.

vacuum-evaporated thin film of aluminium. On abraded quartz the thin coating is punctured over the region of contact and may be photographed on a transmission optical microscope (Fig. 12).

4.1.2. Poisson's ratio

The Hertzian fracture of anisotropic bodies is extremely complicated even for the simple cubic case [39]. Lawn indicates that the computation of Hertzian cone crack paths in diamond [35] gives unreliable results and our experience with quartz indicates the same. It may be more instructive to consider a model for anisotropic fracture based on an elastic continuum.

The two material variables in Equation [5] are ν and γ. For quartz γ is essentially independent of orientation since the cleavage planes are ill-defined. However, ν varies greatly [40] and principally accounts for the very high variation in P_c observed from plane to plane. A simple modification of isotropic theory, which takes into account the angular variation of Poisson's ratio in the plane of indentation as a function of azimuth angle ϕ gives

$$\sigma = \frac{(1 - 2\nu(\phi))}{2} \frac{P}{\pi y^2} \cdot \qquad (3a)$$

Since Hertzian fracture is initiated from planes approximately perpendicular to the plane of indentation, it is necessary to know accurately the value of ν for the direction within the plane corresponding to the "initiation tangent" of the ring crack. This may be a useful starting point for theoretical models, since the ability of a material to crack under contact loading depends on its ability to translate contact compressive forces into remote tensile stresses and this ability is affected by elastic anisotropy. For this reason average values of ν corresponding to small viations in ϕ over the initiation region of the ring cracks are included in Table II. The importance of Poisson's ratio in the contact loading situation has been recognized also for the case of glass [41] in which ν is strain dependent [42], but constant within the plane of indentation.

5. Effect of temperature and environment

The decrease of P_c with temperature in air or N_2 is by no means solely due to the decrease in Young's modulus, which remains virtually constant until the $\alpha \rightarrow \beta$ transition is approached (Fig. 5). There is a very significant difference between the behaviour in air and the drier environment of nitrogen which suggests that the fracture behaviour of quartz is strongly influenced by the presence of water. This occurs in two separate forms, in the external environment in the vicinity of the contact area (referred to as "extrinsic" water), and water present within the crystal as a result of hydrothermal growth during manufacture ("intrinsic" water). The role of these two sources of OH^- contamination will be discussed in turn.

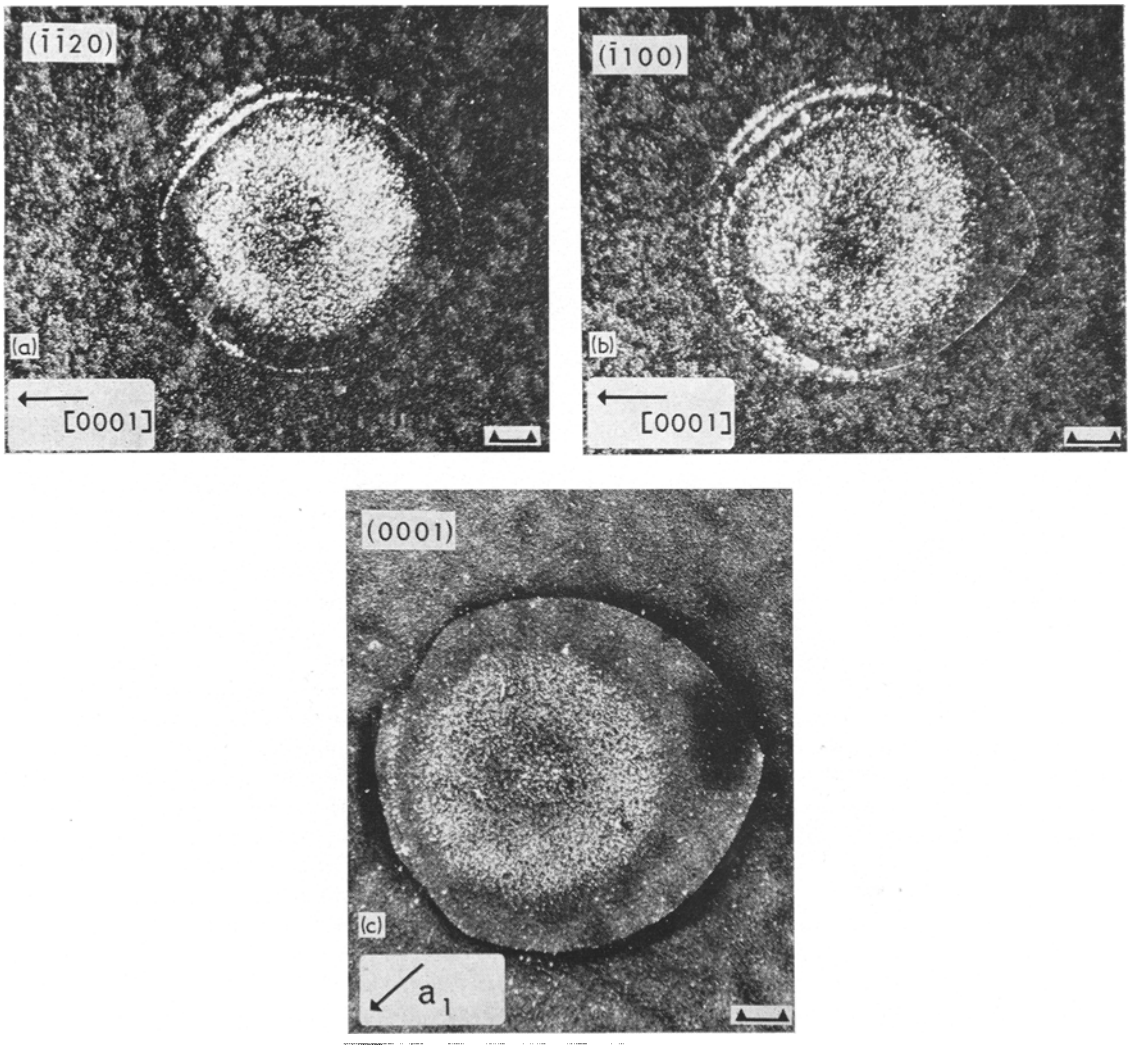

Figure 12 Hertzian ring cracks on (1̄1̄20), (1̄100) and (0001) photographed through a thin film of aluminium to reveal the position of the circle of contact. Marker = 0.1 mm. The contact area extends completely over the light circular region contained within the ring crack.

5.1. Extrinsic water

The influence of water vapour on the mechanical behaviour of silica-based glass has been known for several years and the phenomenon of static fatigue has been the subject of many investigations. The work of Wiederhorn [43, 44] and of Schönert [45] is of particular interest. Basically the highly stressed material at the region of the crack tip chemically reacts with water and as a result a reduction in silicon-oxygen bond strength occurs. This reaction introduces kinetic factors into the dynamical effects at the crack tip. The slower the crack propagates, the more time there is for the reaction to take place and the greater is the reduction in measured fracture toughness. Thus γ is velocity-dependent, increasing as the crack velocity increases until the crack travels too fast for the reaction to occur.

This is believed to be the primary mechanism behind the observed environmental effects presented in Figs. 6 and 7. It is worth remarking that the Hertzian test is very sensitive to changes in environment whereas the three-point bend test is not. This may be attributed to the absolute initial crack size which initiates the final fracture event. The cracks in Hertzian tests are only a few microns in length before instability and thus increase by a significant proportion of their

length while accelerating in a stable manner. In the pre-cracked bend test however, the initial crack is usually of the order of a few millimetres long and so the change in absolute crack size due to stable (slow) crack growth prior to instability is not sufficient to influence the fracture load. This commends the Hertzian test as being extremely useful for measuring environmentally modified changes in γ which might have gone undetected if a more conventional form of fracture test had been used.

The stress-corrosion effects of water have been quantified by Wiederhorn [44] using a semi-empirical thermally activated velocity equation. It would be difficult to make appropriate measurements for quartz because of its cleavage tendencies, but it is reasonable to expect that it will behave very similarly to amorphous silica for which data are available.

It is also apparent from Figs. 8 and 9 that the extrinsic water influences the fracture behaviour over the whole range of temperature investigated. Water is strongly adsorbed onto the quartz surface and is still effective up to the maximum temperature investigated. The attempts to produce an atmosphere free of water by using dry nitrogen are probably only partially successful in that the initial moisture adsorbed on the surface can never be completely removed.

5.2. Intrinsic water

Although no evidence for intrinsic water-weakening was found during microhardness testing, the humps in the basal plane data of Fig. 8 imply a change in mechanism and it is tempting to suggest that this marks the beginning of the regime in which intrinsic water-softening takes over from the extrinsic effects predominant at lower temperatures. It is possible that in nitrogen, intrinsic weakening is revealed more clearly because the environment is failing to replace the water desorbed from the abraded surface during heating. Experiments are currently in progress at the University of New South Wales under vacuum conditions and it is hoped that intrinsic and extrinsic effects may be more thoroughly separated.

The low bond strength of the Si-OH . . . HO-Si complex means that the generation and propagation of dislocation kinks [5] is associated with *partially ruptured* bonds. For the case of fracture, an isolated crack is propagated by the complete rupture of the bonds at the crack tip. The activation energy for bond-breaking may be reduced in the presence of a stress, such as that experienced by an abraded crack under the action of the stress field due to Hertzian contact. Weber and Goldstein [46] have shown that the stress-enhanced diffusion causes Na^+ ions to migrate to crack tips in glass and thus cause substantial weakening in the vicinity of the most highly strained bonds. A similar mechanism may take place in quartz in which OH^- ions diffuse rapidly in regions of high local strain. In Hertzian testing the agglomeration of OH^- ions via kink motion will probably be reflected in a lower instability load since the stress-relaxation mechanism (irreversible deformation at the crack tip) is of itself supplying the corrosive medium.

Some additional experiments revealed that intrinsic water appears to influence fracture behaviour from room temperature upwards. Both natural and synthetic quartz crystals were annealed at various temperatures before being Hertzian-tested at *room temperature*. The results are presented in Fig. 13. The fracture loads were observed to increase quite significantly for the synthetic crystals, whereas there was a relatively small effect for the natural crystals. The synthetic specimens became visibly cloudy as the annealing temperature was raised as a result of intrinsic water condensing in the form of microscopic bubbles. This had the effect of denuding the lattice of water and consequently reduced the availability of a potential weakening source. The increase in P_c at room temperature after annealing implies that stress-enhanced diffusion of OH^- takes place at ambient temperatures. It is remarkable that intrinsic water is still effective well below the softening temperature observed by Griggs (Fig. 3). The microhardness experiments of Nadeau [3] on natural quartz complement our observation of intrinsic water mobility in two ways – firstly, a very "heavy" anneal (24 h at 1400°C) was found to increase the room-temperature microhardness by about 40%, and secondly, annealing increased the hardness over the entire temperature range *and* removed the weakening effect normally observed above 500°C.

The fracture load tends to a very small value as the transition temperature is approached (Figs. 8 and 9). This trend in P_c appears to manifest itself well before the rapid reduction in elastic moduli. Reference has already been made to Schlössin's proposal [36] that cone fracture is preceded by the formation of Dauphiné twins.

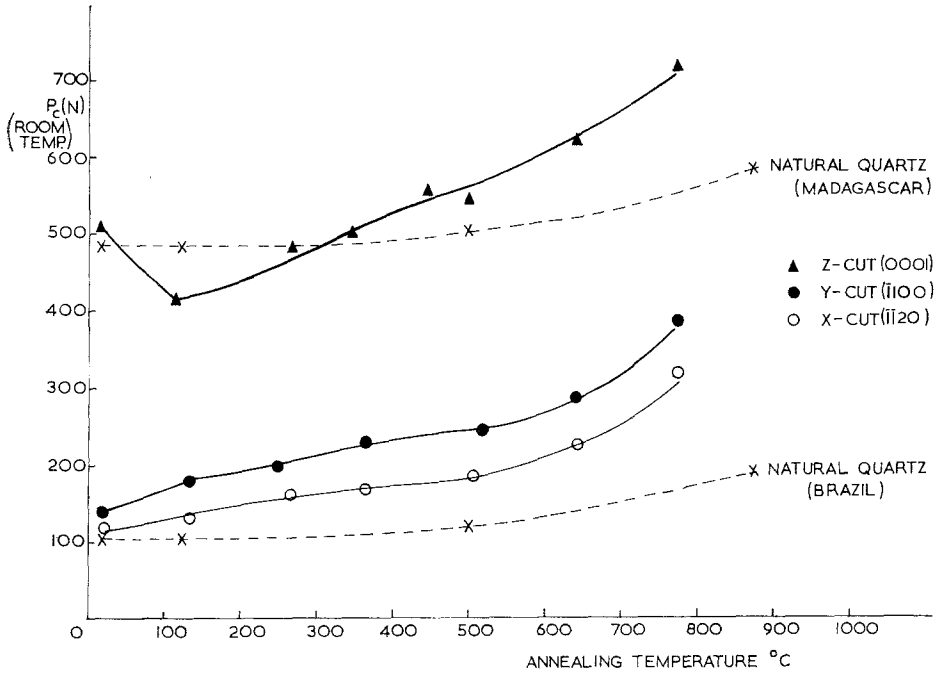

Figure 13 Results of annealing experiments on natural and synthetic quartz. Abscissa is the temperature at which each specimen was annealed for 1 h, ordinate is the room temperature value of P_c after furnace cooling.

The external (mechanical) driving force required to nucleate a twin near the surface may fall to zero at a temperature where the crystal is on the point of changing its structure. It is difficult to determine the effect of twins on fracture behaviour and this has yet to be experimentally verified.

6. Conclusions

Under conditions of contact loading quartz may become extremely weak and is temperature and environment-sensitive. Below 520°C the hardness of synthetic quartz is unaffected by intrinsic water. These results of fracture and deformation experiments support the intrinsic hydrolytic weakening phenomenon in quartz, which may occur at low temperatures due to stress-enhanced diffusion. The role of OH^- ions in the silica lattice is not clarified but appears to be markedly affected by annealing.

Poisson's ratio is a very important parameter in Hertzian fracture experiments and largely accounts for the great variation in P_c observed for quartz planes of different orientation at constant temperature. Extrinsic water, either supplied by the environment or locked into the surface during abrasion, may induce slow crack growth and reduce the fracture toughness.

The fracture toughness of synthetic quartz under conditions of rapid crack propagation from a large crack in three-point loading is 11.5 ± 1.5 Jm^{-2} in air at room-temperature.

Acknowledgements

This work was supported from a research project financed by the Rio-Tinto Zinc Corporation Ltd and Consolidated Gold Fields Ltd. We wish to acknowledge discussions with Dr B. R. Lawn (University of New South Wales), Professor R. W. Cahn, Mr J. W. Heavens (Pilkington Brothers Ltd) and Dr C. A. Brookes (Exeter University) who indented and analysed some Knoop specimens of quartz. We would also like to thank Professor R. W. Cahn for providing laboratory facilities and Mr R. C. Bennett for technical help.

References

1. J. H. WESTBROOK, *J. Amer. Ceram. Soc.* **41** (1958) 433.
2. W. F. BRACE, *J. Geol.* **71** (1963) 581.
3. J. S. NADEAU, *J. Amer. Ceram. Soc.* **53** (1970) 568.
4. D. T. GRIGGS and J. D. BLACIC, *Science* **147** (1965) 292.
5. D. T. GRIGGS, *Geophys. J. Roy. Astr. Soc.* **14** (1967) 19.

6. C. H. SCHOLZ and R. J. MARTIN, *J. Amer. Ceram. Soc.* **54** (1971) 474.
7. R. D. BAËTA and K. H. G. ASHBEE, *Phil. Mag.* **15** (1967) 931.
8. *Idem, ibid* **22** (1970) 601 and 625.
9. H. C. HEARD and N. L. CARTER, *Amer. J. Sci.* **267** (1968) 1.
10. J. M. CHRISTIE, H. C. HEARD, and P. N. LA MORI, *ibid* **262** (1964) 26.
11. R. D. BAËTA and K. H. G. ASHBEE, *Amer. Mineral.* **54** (1969) 1551 and 1574.
12. A. V. SCHUBNIKOV and K. ZINSERLING, *Z. Krist.* **83** (1932) 243.
13. F. D. BLOSS, *Amer. J. Sci.* **255** (1957) 214.
14. W. F. BRACE and J. B. WALSH, *Amer. Mineral* **47** (1962) 1111.
15. C. FRONDEL, (Ed.), "Dana's System of Mineralogy" Vol. III (Silica Minerals) (John Wiley, New York, 1962).
16. A. KATS, *Philips Res. Repts.* **17** (1962) 133.
17. K. L. JOHNSON, *J. Mech. Phys. Solids* **18** (1970) 115.
18. C. A. BROOKES, J. B. O'NEILL, and B. A. W. REDFERN, *Proc. Roy. Soc.* **322A** (1971) 73.
19. D. M. MARSH, *ibid* **279A** (1964) 420.
20. E. W. TAYLOR, *Min. Mag.* **28** (1949) 718.
21. K. W. PETER, *J. Non-Cryst. Solids* **5** (1970) 103.
22. C. PETERS, *Fortschr. Chem. Forsch.* **1** (1950) 613 (quoted in [8]).
23. D. TABOR, "The Hardness of Metals" (Clarendon Press, Oxford, 1951) 175 pp.
24. G. J. F. MACDONALD, *Amer. J. Sci.* **254** (1956) 713.
25. C. A. BROOKES, private communication.
26. H. H. SCHLÖSSIN, *Phil. Mag.* **12** (1965) 467.
27. N. E. W. HARTLEY, Thesis, University of Sussex, 1971.
28. W. F. BROWN and J. E. SRAWLEY, Chap. 5 in A.S.T.M. Spec. Tech. Publn. No. 381 (1965).
29. T. R. WILSHAW, *Brit. J. Appl. Phys. D* **4** (1971) 1567.
30. S. M. WIEDERHORN, A. M. SHORB, and R. L. MOSES, *J. Appl. Phys.* **39** (1968) 1569.
31. F. C. FRANK and B. R. LAWN, *Proc. Roy. Soc.* **299A** (1967) 291.
32. B. R. LAWN, *ibid* **299A** (1967) 307.
33. F. B. LANGITAN and B. R. LAWN, *J. Appl. Phys.* **40** (1969) 4009.
34. F. C. ROESLER, *Proc. Phys. Soc.* **69B** (1956) 981.
35. B. R. LAWN, *J. Appl. Phys.* **39** (1968) 4828.
36. H. H. SCHLÖSSIN, Univ. of the Witwatersrand, Chamber of Mines Research Project No. 122/65 (303/65) Report (1968); (unpublished).
37. M. V. KLASSEN-NEKLYUDOVA, "Mechanical Twinning of Crystals", Transl. from the Russian (Consultants Bureau, New York, 1964).
38. P. B. WITHERS, unpublished research.
39. J. R. WILLIS, *J. Mech. Phys. Solids* **14** (1966) 163.
40. W. G. CADY, "Piezoelectricity" (McGraw-Hill, New York, 1946), Chap. 4, 806 pp.
41. B. R. LAWN, T. R. WILSHAW, and N. E. W. HARTLEY, to be published.
42. F. P. MALLINDER and B. A. PROCTER, *Phys. & Chem. Glasses* **5** (1964) 91.
43. S. M. WIEDERHORN, *J. Amer. Ceram. Soc.* **50** (1967) 407.
44. S. M. WIEDERHORN and L. H. BOLZ, *ibid* **53** (1970) 543.
45. K. SCHÖNERT, H. UMHAUER, and W. KLEMM, in "Fracture", Paper 41 of Proc. 2nd Internat. Conf. on Fracture, Brighton, April 1969 (Chapman and Hall, London, 1969).
46. N. WEBER and M. GOLDSTEIN, *J. Chem. Phys.* **41** (1964) 2898.
47. A. PERRIER and R. DE MANDROT, *Mem. Soc. Vaud. des Sciences Nat.* **1** (1923) 333.
48. L. A. THOMAS and W. A. WOOSTER, *Proc. Roy. Soc.* **208A** (1951) 43.

Received 27 June and accepted 20 July 1972.